MOL#42002

Title Page

Antitumorigenic Effects of Peroxisome Proliferator-Activated Receptor-γ (PPARγ) in Non-small Cell Lung Cancer Cells (NSCLC) are Mediated by Suppression of COX-2 via Inhibition of NF-κB *

Yvette Bren-Mattison[1], Amy M. Meyer[1], Vicki Van Putten, Howard Li, Katherine Kuhn, Robert Stearman, Mary Weiser-Evans, Robert A. Winn, Lynn E. Heasley, and Raphael A. Nemenoff

Department of Medicine, University of Colorado Health Sciences Center

Denver, CO 80262

MOL#42002

Running Title Page

Running Title: PPARγ Inhibits Lung Tumorigenesis by Inhibition of COX-2

Corresponding Author:
Raphael Nemenoff
Division of Renal Diseases and Hypertension,
Dept. of Medicine, University of Colorado Health Sciences Center,
Box C-281,
4200 E. 9th Ave., Denver, CO 80262.
Tel.: (303) 315-6733; FAX: (303) 315-4852;
E-mail: Raphael.Nemenoff@UCHSC.edu.

Document Statistics

Text pages: **26**

Tables **none**

Figures **7**

References **39**

Abstract **227 words**

Introduction **636 words**

Discussion **1231 words**

Abbreviations: PPAR, peroxisome proliferator-activated receptor; NSCLC, non-small cell lung cancer; TZD, thiazolinedione; PPAR-RE, PPAR response element; NSAIDs, non-steroidal antiinflammatory drugs; COX-2, cyclooxygenase-2; PGE$_2$, prostaglandin E$_2$.

MOL#42002

Abstract

Pharmacological activators of peroxisome proliferator-activated receptor-γ (PPARγ) inhibit growth of non-small cell lung cancer (NSCLC) cell lines in vitro and in xenograft models. Since these agents engage off-target pathways, we have assessed the effects of PPARγ by overexpressing the protein in NSCLC cells. We previously reported that increased PPARγ inhibits transformed growth and invasiveness, and promotes epithelial differentiation in a panel of NSCLC expressing oncogenic K-Ras. These cells express high levels of COX-2 and produce high levels of PGE_2. The goal of these studies was to identify the molecular mechanisms whereby PPARγ inhibits tumorigenesis. Increased PPARγ inhibited expression of COX-2 protein and promoter activity, resulting in decreased PGE_2 production. Suppression of COX-2 was mediated through increased activity of the tumor suppressor PTEN, leading to decreased levels of phospho-Akt and inhibition of NF-κB activity Pharmacological inhibition of PGE_2 production mimicked the effects of PPARγ on epithelial differentiation in 3-dimensional culture, and exogenous PGE_2 reversed the effects of increased PPARγ activity. Transgenic mice overexpressing PPARγ under the control of the surfactant protein C promoter had reduced expression of COX-2 in Type II cells, and were protected against developing lung tumors in a chemical carcinogenesis model. These data indicate that high levels of PGE_2 as a result of elevated COX-2 expression are critical for promoting lung tumorigenesis, and that the antitumorigenic effects of PPARγ are mediated in part through blocking this pathway.

3

Introduction

Peroxisome proliferator-activated receptor-γ (PPARγ) is a member of the nuclear-hormone-receptor superfamily, and was initially demonstrated to have important roles in lipid metabolism and adipose differentiation (see (Berger and Moller, 2002) for review). PPARγ binds as a heterodimer with the retinoic acid X receptor (RXR). These heterodimers, complexed with either co-activators or co-repressors, bind to specific PPAR response elements in the promoter regions of their target genes. PPARγ is activated by polyunsaturated fatty acids and eicosanoids, as well as by the class of thiazolidinediones (TZDs). Activation of individual PPAR isoforms has been implicated in many types of cancer, including breast, colon, and prostate (see (Feige et al., 2006) for review). In lung cancer, several studies, including work from our laboratory, have demonstrated that pharmacological activation of PPARγ can inhibit growth of lung cancer cells (Wick et al., 2002). In samples from human lung tumors, decreased expression of PPARγ was correlated with poor prognosis (Sasaki et al., 2002). In a separate study, well-differentiated adenocarcinomas exhibited a greater frequency of PPARγ-positive cells compared to poorly differentiated samples (Theocharis et al., 2002). Prostaglandins are a family of bioactive lipid mediators, which are derived through metabolism of arachidonic acid (AA). Release of AA from membranes is mediated through the action of phospholipase A_2, primarily the cytosolic intracellular form designated as $cPLA_2$. Cyclooxygenases (COX) convert free AA to prostaglandin H (PGH_2), which is the precursor for other prostaglandins and thromboxane. Two isoforms of COX have been described. COX-1 is constitutively expressed in most cell types, and thought to be responsible for prostaglandin production involved in maintenance of vascular tone. COX-2, normally expressed at low or undetectable levels in most cells, is rapidly induced by mitogenic or inflammatory signals through transcriptional activation. Conversion of PGH_2 to downstream eicosanoids is mediated by expression of specific terminal synthases. In NSCLC the major eicosanoid produced is prostaglandin E2 (PGE_2) produced through microsomal PGE_2 synthase (mPGES). A large body of evidence indicates that

increased prostaglandin production contributes to tumorigenesis. COX-2 has been shown to be constitutively up-regulated in various cancers including; colon, breast and lung, and targeted over-expression of COX-2 is sufficient to cause mammary tumorigenesis in transgenic mice (Liu et al., 2001). Elevated levels of PGE_2 are found in lung cancer tissue compared with normal lung tissue with consistently higher production in adenocarcinomas (McLemore et al., 1988). Constitutively high levels of PGE_2 production are observed in a subset of non-small cell lung cancer (NSCLC), and correlate with expression of oncogenic K-Ras (Heasley et al., 1997). This is a consequence of expression of $cPLA_2$ and COX-2. NSAIDs, which inhibit COX isoforms, block the growth of cancer cells *in vitro*, and inhibit tumor growth *in vivo* (Heasley et al., 1997; Hida et al., 1998). The mechanisms whereby COX-2-derived PGE_2 promotes tumorigenesis and progression are not well understood but may involve stimulating growth, preventing apoptosis, increasing cell motility and adhesion, inducing angiogenesis and inhibiting immune surveillance.

Since TZDs have been reported to engage off-target effectors, it has been difficult to define the specific pathways regulated by PPARγ. We have employed a molecular approach to overexpress PPARγ in NSCLC, resulting in levels of activity comparable to stimulation of untransfected cells with TZDs (Bren-Mattison et al., 2005). Overexpression of PPARγ in human non-small cell lung cancer (NSCLC) cell lines did not have a major effect on cell proliferation, but had selective inhibitory effects on anchorage independent growth and metastasis, and promoted epithelial differentiation in 3-dimensional cultures (Bren-Mattison et al., 2005). However, the mechanisms underlying these effects have not been identified. The goal of the present study was to determine whether the anti-tumorigenic effects of PPARγ were mediated through regulation of the COX-2 pathway in vivo and in NSCLC. We report here that increased PPARγ activity inhibits COX-2 expression through inhibition of Akt signaling resulting in reduced NF-κB activity.

Materials and Methods

Materials   T0070907 (PPARγ inhibitor) was from Cayman Chemical Co (Ann Arbor MI). Sulindac sulfide was from ICN Biochemical (Aurora OH). IKK-Inhibitor VII was from Calbiochem. NF-κB assay kit (TransAM NF-κB Chemi kit) was from Active Motif (Carlsbad, CA).

Cell culture and 3-dimensional culture   H2122 and A549 cells, both human lung adenocarcinoma cell lines were obtained from the University of Colorado Health Science Center Tissue Culture Core. Cells were maintained in RPMI containing 10% fetal bovine serum. H2122-LNCX and H2122-PPARγ stable clones have been previously described (Wick et al., 2002). Cells were grown in three-dimensional basement membrane cultures according to Debnath et al.(Debnath et al., 2003) with the following modifications: growth factor reduced Matrigel (BD Bioscience) was combined in a 1:1 ratio with full serum medium (RPMI +10% FCS). 80 µl was added to each well of an eight-well glass slide chamber (LAB-TEK, Nalge Nunc International) and allowed to solidify for 2 hours in a 37^0C incubator. Cells were trypsinized, counted and diluted to 25,000 cells/ml. A 20% Matrigel solution was prepared in full serum medium. The cell suspension was combined in a 1:1 ratio with the 20% Matrigel solution and 200 µl of this mixture was added to each well for a final concentration of 5000 cells/well in 10% Matrigel. Cells were fed with 4% Matrigel (in full serum medium) every other day for a term of 8-10 days of culture. For experiments with exogenous PGE_2 cells were incubated with 5 µM; this higher concentration was chosen for longer experiments NSCLC express 15-hydroxyprostaglandin dehydrogenase (15-PGDH) which rapidly degrades PGE_2 (Hazra et al., 2007). A similar range of concentrations has been used by other investigators (Casibang et al., 2001; Huang and Cabot, 1990), even for acute stimulation of lung cancer cells. Control cells received vehicle (0.1% DMSO).

Promoter Transfections. Cells were plated in 60 mm dishes at approximately 600,000/dish. Promoter transfections were performed using 1 μg each of the indicated luciferase promoter construct and CMV-β-gal using lipofectamine (Invitrogen, Carlsbad CA) as previously described (Wick et al., 2002). Total DNA content was matched for each sample using the appropriate empty vector. Cells were harvested in reporter lysis buffer (Promega, Madison WI), and luciferase normalized to β-galactosidase determined.

Indirect immunofluorescence Cells grown in 3-D culture were immunostained as previously described with some modifications (Debnath et al., 2003) Briefly, cells were fixed with 2% paraformaldehyde in phosphate buffered saline (PBS) for 20 minutes at room temperature, permeabilized with 0.5% Triton X-100, and rinsed 3 times with 100mM glycine. The cells were then incubated in primary block (7.7 mM NaN_3, 0.1% bovine serum albumin, 0.2% Triton X-100, 0.05% Tween-20, and 10% goat serum in PBS) for 1 hour at room temperature. Following a 30-minute incubation in secondary block (primary block plus 20 μg/ml goat anti-mouse $F(ab')_2$ fragment (Jackson ImmunoResearch)), cells were incubated with primary antibodies; cleaved Caspase-3 (at 1:50, Cell Signaling Technology), and E-cadherin (at 1:100, BD Biosciences) over night at room temperature. Cells were rinsed 3 times prior to incubation with secondary antibodies (Alexa Fluor 488 goat anti-mouse, Alexa Fluor 568 goat anti mouse, Alexa Fluor 488 goat anti-rabbit, and Alexa Fluor 568 goat anti-rabbit, all used at 1:250, Molecular Probes). Cells were mounted using Vectashield fluorescent mount medium containing 4', 6-diamidino-2-phenylindole (Vector Laboratories). At least 20 aggregate structures were examined in each of three independent experiments; representative images are shown. Structures grown in 3-D matrices were imaged and acquired on a Zeiss 510 Meta NLO confocal microscope (Carl Zeiss Microimaging, Thornwood, NY) and analyzed using Zeiss Image Examiner software.

Immunoblotting Cells grown in 2-D culture were lysed in cold RIPA buffer (10mM TrisHCl, 150 mM NaCl, 1% NaDOC, 1% Triton X-100, 0.1% SDS) containing protease inhibitors, centrifuged at

10,000xg for 5 minutes, and the supernatant saved. Cells grown in 3-D Matrigel were first isolated using BD Cell Recovery Solution (BD Biosciences) as per manufacturer's instructions. This involves dissociation of the Matrigel matrix by enzymatic digestion with Dispase. These cells were then processed as the cells grown in 2-D culture. Protein was quantitated using Bio-Rad Protein Assay reagent (Bio-Rad). Protein samples were run on precast 4-20% Gradient Tris-HCl gels (Bio Rad). Antibodies against COX-2 and PPARγ were from Cayman (An n Arbor MI). Antibodies against Akt were from Cell Signaling (Danvers, MA). Blots were visualized by enhanced chemiluminescence, and changes in expression normalized to β-actin expression were determined by densitometry using at least three independent experiments.

Prostaglandin E$_2$ Assay PGE$_2$ levels were measured by ELISA as per manufacturer's instructions (Prostaglandin E$_2$ EIA Kit- Monoclonal; Cayman Chemical Company, Ann Arbor, MI). Briefly, cells were grown in 10 cm plates to 90% confluency. Medium was removed, plates were washed with Hanks buffered saline, and new medium was added. 1ml of this medium was immediately removed and assayed for PGE$_2$ levels to establish the "zero" time point. One hour later a second 1ml aliquot of medium was removed and assayed for PGE$_2$ levels. All samples were analyzed according to manufacturer's recommended protocol.

PTEN Activity Measurements PTEN was immunoprecipitated from cell lysates using anti-PTEN antibody from Cell Signaling (Danvers, MA) and Protein A-sepharose. Activity was measured in the immunoprecipitate using PIP$_3$ as a substrate for 45 minutes at 37^{0}C following the procedure described in the Echelon kit, and phosphate generated in the supernatant was quantified using the generic phosphatase assay kit from Echelon (Salt Lake City, UT).

Construction of SP-C/PPARγ transgene The 3.7 hSP-C/SV-40 plasmid was a generous gift from Dr. Jeffrey A. Whitsett (Children's Hospital Medical Center, Cincinnati, Ohio). This pUC 18 plasmid contains the 3.7-kb flanking sequence of the human SP-C promoter in addition to the SV-40 small T intron as a polyadenylation signal. The full-length human PPARγ1 cDNA was cut and cloned into the *SalI/EcoRI* site of the hSP-C/SV-40 plasmid by blunt end ligation, creating the SP-C promoter- PPARγ cDNA fusion gene. The proper cloning orientation of our construct was confirmed by direct sequence analysis. Transgenic mice were developed in a FVB/N strain by pronuclear injections of the linearized construct. Transgenic mice were genotyped by analyzing genomic DNA isolated from tail biopsies with the DNeasy Tissue Kit according to the manufacturer's instructions (QIAGEN Inc., Santa Clarita, California). PCR was performed on genomic DNA using primers spanning the 400-bp segment of the SV-40 small T intron to detect the presence of the transgene (sense primer: 5'-TGTGAAGGAACCTTACTTCTGTGG-3'; antisense primer: 5'-TGGACAAACCACAACTAGAATGCAC-3'). All mice were propagated as heterozygous transgenic mice by breeding with wild-type FVB/N mice.

Mouse Carcinogenesis protocols FVB/N mice 8-12 weeks of age were maintained on a standard, antioxidant-free laboratory chow (Lab Diet; PMI Nutrition International, St. Louis, MO) and given food and water *ad libitum*. Animals were kept on cedar-free bedding with a 12-h light/dark cycle in a climate-controlled animal facility. A single urethane (Sigma Chemical Co.) dose (1mg/g mouse weight), dissolved in normal saline, was administered intraperitoneally and animals were sacrificed 20 weeks later. Tumors were enumerated in fresh lungs under a dissection microscope. All tumors were dissected from the lung parenchyma. The diameter of individual tumors was measured using digital calipers. The genetic identity of the mice (PPARγ⁻ or PPARγ⁺) was not revealed until after tumor

multiplicities and sizes were determined. All procedures were performed under a protocol approved by the IACUC at the University of Colorado Health Sciences Center.

Type II cell isolation Type II pneumocytes were isolated from untreated transgenic or wild-type mice as previously described (Corti et al., 1996). Briefly, mice were anesthetized with i.p. injection of phenobarbital (200μl). The abdominal cavity was opened, and mice were exsanguinated by severing the renal artery. The trachea was isolated and cannulated with a 20-gauge luer lock cannula. The diaphragm was cut, and the anterior chest wall and thymus were removed. Lungs were perfused with 10 ml of 0.9% saline via the pulmonary artery using a 21-gauge needle fitted on a 10-ml syringe. Dispase (3 ml) was rapidly instilled through the trachea cannula followed by 0.5 ml of 45°C agarose. The lungs were covered with ice for 2 min. to harden the agarose. After this incubation, the lungs were dissected out from the animals and incubated in a culture tube with 2 ml dispase for 45 min at room temperature. Lungs were then transferred to a 60-mm culture dish containing 7 ml HEPES-buffered DMEM and 100U/ml DNAseI; lung tissue was gently teased apart and minced until only connective tissue was visible, and the cell suspension was filtered through progressively smaller cell strainers (100 and 40 μm) and nylon gauze (20 μm). Cells were collected by centrifugation at 130 xg for 8 min. at 4°C, placed on pre-washed 100-mm culture dishes that had been pre-coated with 42 mg anti-CD45 antibody and 16 mg anti-CD32 antibody in PBS for 24-48 h at 4°C, and incubated for 1.5 h at 37°C. The medium containing type II cells was gently removed from the plates and the cells were collected by centrifugation. Cell pellets were lysed in RIPA buffer (150 mM NaCl, 10 mM Tris, pH 7.2, 0.1% SDS, 1% Triton X-100, 1% deoxycholate, 5 mM EDTA, protease inhibitors), centrifuged at 10,000 x g for 10 min., and matched for protein. For EIA and LCMS analysis of PGE2 levels, the collected cells were washed several times with 1X PBS. The cells were then suspended in 1 mL of complete medium (DMEM plus 10% fetal calf

serum) and incubated at 37°C for 30 min. The medium was collected and centrifuged at 10,000 x g for

10 min. The supernatant was diluted 1:3 in methanol for analysis of PGE2 levels and the cell pellets

were processed for immunoblotting as described above.

MOL#42002

Results

PPARγ inhibits COX-2 expression and PGE2 production in NSCLC.

H2122 cells are a human adenocarcinoma cell line which express elevated levels of COX-2 and produces high levels of PGE_2 (Heasley et al., 1997). We have previously shown that increased PPARγ activity promotes epithelial differentiation of these cells in 3-D culture (Bren-Mattison et al., 2005). To examine whether these effects of PPARγ are mediated through changes in prostaglandin pathways, we compared expression of enzymes in this pathway in H2122 cells stably overexpressing PPARγ (H2122-PPARγ) or control cells transfected with empty vector (H2122-LNCX). Expression of $cPLA_2$ and COX-2 were significantly decreased in H2122-PPARγ cells compared to H2122-LNCX cells (Fig. 1A) or untransfected H2122 cells (data not shown); mPGES levels were not significantly changed. Desnitometry of three independent experiments showed a 50% decrease in $cPLA_2$ expression and a 72% reduction in COX-2 expression. We have also performed expression profiling of these cells using Affymetrix microarrays. Both $cPLA_2$ and COX-2 were called as "decreased" on the arrays ($cPLA_2$ by 60% and COX-2 by 75%), whereas expression of mPGES was predicted to be moderately increased (20%, data not shown). Consistent with these data, H2122-PPARγ cells exhibited a marked decrease in production of PGE_2 compared to H2122-LNCX cells (Fig. 1B). This effect was reversed by a specific pharmacological inhibitor of PPARγ, T0070907 (T007)(Lee et al., 2002). We tested whether the effects of PPARγ on COX-2 were mediated at the transcriptional level by using a COX-2-Luciferase (COX-2-Luc) reporter construct that contains approximately 500bp of the human COX-2 promoter ligated to a luciferase reporter. Activity of this promoter construct is strongly induced by oncogenic Ras in lung epithelial cells (Van Putten et al., 2001). PPARγ-H2122 showed a 70% decrease in promoter activity as compared to control cells (Fig. 1C). This inhibition of COX-2 promoter activity was also completely

12

reversed by the PPARγ inhibitor.   Similar results were found in a second NSCLC adenocarcinoma cell line, A549, which also expresses high levels of COX-2 (Heasley et al., 1997)(see Fig. 5).

Effects of PPARγ on epithelial differentiation in 3-dimensional culture are mediated by inhibition of PGE$_2$

We have previously shown that PPARγ promotes an epithelial-like cell morphology in NSCLC when grown in 3-dimensional Matrigel culture (Bren-Mattison et al., 2005). Non-transformed epithelial cells form hollow, polarized acinar structures, where cells not in contact with the matrix undergo apoptosis (Debnath et al., 2003).   To determine the role of PGE$_2$ production in this process, cells grown in 3-D culture were exposed to sulindac sulfide, a COX inhibitor. The concentration of sulindac sulfide used in these experiments (5 μM) inhibits PGE$_2$ production greater than 90%, but does not activate PPARγ (Wick et al., 2002)(see Supplementary Fig. 1).   Polarized acinar structures were defined by positive E-cadherin staining in the basolateral membrane, and luminal cell death indicated by positive cleaved caspase 3 staining. Consistent with our previous findings (Bren-Mattison et al., 2005), H2122-LNCX cells formed disorganized aggregates, (Fig. 2A,E), while H2122-PPARγ cells form ordered structures (Fig. 2B,F).   In contrast to non-transformed epithelia, cells in the center do not undergo apoptosis, suggesting that while these cells are more differentiated, they are still structurally distinct from non-transformed epithelial cells.   Exposure of H2122-LNCX to low concentrations of sulindac sulfide resulted in formation of ordered acinar structures similar to those seen in H2122-PPARγ cells (Fig. 3C,G). In fact, regions in the center of the structures stained positive for activated caspase 3 (red color in 3G). Conversely, addition of exogenous PGE$_2$ (5 μM) to H2122-PPARγ cells caused these cells to revert to a disordered aggregate (Fig. 2D,H), similar to what is seen in H2122-LNCX cells.   These

data strongly suggest that inhibition of PGE$_2$ production is critical for formation of differentiated

structures in 3-D by PPARγ.

PPARγ Inhibits COX-2 Expression via an NF-κB-Dependent Mechanism

Several regions of the COX-2 promoter have been shown to be critical for regulation, including

CRE, NF-IL6, and NF-κB consensus binding sites (Reddy et al., 2000). Since previous reports have

demonstrated effects of PPARγ on NF-κB (Keshamouni et al., 2005), we examined whether regulation

of COX-2 expression in H2122 cells was mediated through control of NF-κB. The effects of PPARγ on

NF-κB were assessed using a plasmid containing 3 consensus NF-κB binding sights upstream of a

luciferase reporter.   Overexpression of PPARγ in H2122 cells decreased NF-κB activity by

approximately 50% (Fig. 3A). This decrease was reversed by exposure to the PPARγ inhibitor T007.

Changes in NF-κB activity were confirmed by quantitation of nuclear NF-κB protein by ELISA (see

Methods). Nuclear extracts were prepared from H2122-PPARγ and H2122-LNCX cells and NF-κB

binding quantitated using the TransAM NF-κB Chemiluminescence kit from Active Motif. Nuclear NF-

κB activity was decreased by approximately 70% in H2122-PPARγ cells compared to N2122-LNCX

(Fig. 3B).

To directly assess the role of PPARγ on NF-κB activity in control of the COX-2 promoter,

H2122 cells were co-transfected with the COX-2 promoter construct along with an expression plasmid

encoding a dominant-negative IκB (DN-IκB), in which the amino terminal containing regulatory

phosphorylation sites has been deleted. Expression of DN-IκB decreased NF-κB activity by greater

than 90% (Fig. 4A; left panels). Importantly, COX-2 promoter activity was decreased by 50% in the

presence of DN-IκB (Fig. 4A right panels). These findings were confirmed using a pharmacological

inhibitor of NF-κB, which acts by inhibiting Iκ-B kinase, IKK (IKK Inhibitor VII, Calbiochem).

MOL#42002

Exposure of H2122 cells to this agent decreased NF-κB activity in a dose-dependent manner, with an IC50 of less than 5 μM (Fig. 4B). At a concentration of drug that inhibited NF-κB activity by ~70%, COX-2 protein expression was decreased by approximately 70% (Fig. 4C). Thus, regulation of NF-κB is a dominant signaling pathway controlling the expression of COX-2 in H2122 cells. We confirmed the regulation of NF-κB in a second NSCLC line, A549. Similarly to what was observed in H2122 cells, overexpression of PPARγ decreased NF-κB activity (Fig. 5A) and decreased COX-2 promoter activity (Fig. 5B).

PPARγ Effects on NF-κB and COX-2 are Mediated through Increased Activity of PTEN and Inhibition of Phospho-Akt

Several studies have demonstrated that constitutive activation of NF-κB in tumor cells is mediated through activation of Akt, although the precise mechanisms have not been well defined (Madrid et al., 2000; Romashkova and Makarov, 1999; Sizemore et al., 1999). We therefore examined the role of Akt in mediating the effects of PPARγ. NSCLC expressing oncogenic K-Ras mutations had constitutively high levels of activated, phospho-Akt (p-Akt). In H2122 cells overexpression of PPARγ resulted in marked inhibition of steady state p-Akt levels ,with no change in total Akt levels (Fig. 6A). Treatment of cells with a LY 294002 (10 μM), a PI-3 kinase inhibitor, decreased levels of p-Akt (data not shown). In H2122-LNCX cells, LY 294002 reduced NF-κB-Luc activity by approximately 50%, comparable to activity seen in H2122-PPARγ cells (Fig. 6B); LY 294402 had no further inhibitory effect in H2122-PPARγ cells.

Decreased phospho-Akt could be a result of inhibiting PI-3 kinase activity or increasing the activity of PTEN, which dephosphorylated PIP_3, opposing the actions of PI3K. Since several reports have indicated that PTEN may be a downstream effector of PPARγ (Lee et al., 2006; Teresi et al.,

15

2006), we assessed the effects of PPARγ on PTEN activity in H2122 cells. No consistent effect of PPARγ on PTEN expression was detected by immunoblotting. However, PTEN enzymatic activity as measured by hydrolysis of PIP_3 was significantly increased in the H2122-PPARγ cells compared to H2122-LNCX (Fig. 6C). We propose that decreased phospho-Akt levels in H2122-PPARγ cells is a result of lower PIP_3 levels secondary to increased PTEN activity.

Transgenic mice overexpressing PPARγ have decreased COX-2 expression and are protected against developing lung tumors

To test the relationship between PPARγ and COX-2 expression in vivo, we developed transgenic mice with targeted overexpression of PPARγ in the type II alveolar epithelial cells of the lung, using the surfactant protein C promoter (Keith et al., 2002). Expression of PPARγ in Type II cells isolated from Tg+ animals was markedly increased compared to wild-type littermates (Fig. 7A). Consistent with our observations in H2122 cells, increased PPARγ expression was correlated with decreased expression of COX-2 in these cells (Fig. 7A). The Tg+ mice appeared to have normal lung architecture, and did not display any other abnormalities (data not shown). The role of increased PPARγ in lung tumorigenesis was determined using a well-characterized chemical carcinogenesis protocol, in which mice were injected with a single dose (1g/kg body weight) of urethane, a complete carcinogen (Blaine et al., 2005; Horio et al., 1996; Malkinson, 1998). After 18 weeks, animals were sacrificed, and tumors were evaluated as previously described (Blaine et al., 2005). Tg+ animals had a 75% decrease in tumor number compared to Tg- littermates (Fig. 7B); no difference in mean tumor size was detected (data not shown). Thus, increased *PPARγ* expression inhibits tumorigenesis and COX-2 expression both *in vitro* and *in vivo*. Examination of tumors indicated that there were no significant differences in the histology of tumors from the two groups of mice (Fig. 7C).

Discussion

Data from a number of laboratories, including ours, have demonstrated that activation of PPARγ inhibits the growth of NSCLC in vitro and in vivo (Bren-Mattison et al., 2005; Han and Roman, 2006; Wick et al., 2002). Similarly, studies over the past ten years have shown that inhibition of prostaglandin production has similar inhibitory effects (Rigas and Kashfi, 2005). From the current studies we propose that these two pathways are linked. Specifically, the anti-tumorigenic effects of PPARγ are mediated, at least in part through decreasing production of pro-tumorigenic prostaglandins such as PGE_2. This is mediated through decreased expression of enzymes required for PGE_2 synthesis, specifically $cPLA_2$ and COX-2. In NSCLC in vitro, this decrease in PGE_2 production is both necessary and sufficient for the increased epithelial differentiation observed in the setting of increased PPARγ activity. Pharmacological inhibition of PGE_2 production mimicked the effects of PPARγ on epithelial differentiation in 3D culture, and conversely adding exogenous PGE_2 was sufficient to reverse the effects of PPARγ on epithelial differentiation. In vivo, targeted overexpression of PPARγ to Type II cells also resulted in decreased COX-2 expression in the Type II cells, and this was associated with a marked decrease in lung tumors. The level of protection observed in our study is similar to what has been observed in urethane-injected mice exposed to indomethacin (Moody et al., 2001). These data suggest that PGE_2 production is critical for the initiation of lung tumorigenesis in mice. Further support for that hypothesis comes from studies showing that $cPLA_2$ deficient mice also develop significantly fewer lung tumors in response to the same chemical carcinogenesis model (Meyer et al., 2004). However, data from our laboratory indicate that mice with targeted overexpression of mPGES fail to show alterations in lung tumor formation using the urethane model (Blaine et al., 2005). In that study, increased levels of PGE_2 were observed in the transgenic mice both under basal conditions and following urethane administration. However, wild-type mice had elevated levels of PGE_2 which was

likely mediated by increased COX-2 expression without any change in mPGES. We therefore concluded that the increased PGE$_2$ production by mPGES is necessary but not sufficient to promote tumorigenesis. Alternatively, increased PGE$_2$ production mediated by COX-2 induction is sufficient to promote tumor formation, even without changes in mPGES.

While the COX-2 promoter contains multiple regulatory elements, our data indicate that the inhibitory effects of PPARγ are mediated through NF-κB. Expression of DN-IκB decreased COX-2 promoter activity, and a pharmacological IKK inhibitor decreased COX-2 protein in these cells. Induction of COX-2 expression by growth factors is largely mediated through the CRE element, and involves phosphorylation of c-Jun (Xie and Herschman, 1995). However, other studies have demonstrated a role for NF-κB binding in control of COX-2 transcription. In macrophages, PPARγ ligands inhibited the induction of COX-2 in response to LPS (Inoue et al., 2000), and this involved NF-κB. These effects can be mediated through PPARγ or potentially through off-target effects of these agents. However, other studies have indicated that PPARγ-mediated inhibition of COX-2 expression involves other regulatory elements, suggesting that will be different pathways operative in a cell-specific fashion. The ability of PPARγ to inhibit NF-κB is likely to have wider implications for the biology of these cells. NF-κB has been identified as a critical transcription factor controlling production of a family of cytokines, specifically ELR+CXC cytokines such as IL-6 and L-8. This family of cytokines has been implicated in angiogenesis and metastasis in several types of cancer including lung cancer through direct effects on the cancer cells, or signaling to stromal fibroblasts, endothelial cells and innate immune cells (Strieter et al., 2004). We have observed decreased production of both IL-6 and IL-8 in NSCLC overexpressing PPARγ, and have identified several other cytokines whose is expression is decreased on Affymetrix gene arrays [2]. These data are consistent with studies using pharmacological activators of PPARγ, which also decrease production of these cytokines (Keshamouni et al., 2005). The

role of individual ELR+-CXC cytokines on the transformed growth and differentiation of NSCLC and on specific tumor-stromal interactions is an area of active investigation.

Based on our data we propose that inhibition of NF-κB is mediated through activation of PTEN and subsequent inhibition of Akt activation. Two PPARγ consensus sites have been identified approximately 10 kb upstream of the minimal promoter region of the PTEN gene (Patel et al., 2001), and increased PTEN expression has been observed in response to pharmacological PPARγ activators (Patel et al., 2001). While our data do not support that PTEN is a direct transcriptional target of PPARγ, we propose that the increased PTEN activity in the setting of PPARγ activation is a critical mediator of the anti-tumorigenic effects of PPARγ in lung cancer cells. Further studies demonstrating direct binding of PPARγ to these elements using chromatin immunoprecipitation and mutational analysis of these regions are needed to define the precise mechanism of PTEN regulation. However, it is also possible that PPARγ may regulate PTEN activity through post-transcriptional mechanisms. PTEN activity has been reported to be regulated by phosphorylation/dephosphorylation (see (Gericke et al., 2006) for review). Specifically, dephosphorylation of the protein is associated with increased enzymatic activity, and decreased stability. Increased PPARγ activity could regulate PTEN activity by modifying expression of protein kinases and/or phosphatases which act on PTEN. Activation of PTEN and subsequent inhibition of Akt activation will also have additional effects on NSCLC. Finally, it should be noted that decreased levels of Akt activation could also be a result of inhibition of PI3 kinase by PPARγ. Future studies using siRNA approaches will be required to better define the role of PTEN in the responses of NSCLC.

A recent study has demonstrated that pharmacological activators of PPARγ also decrease PGE$_2$ production in NSCLC (Hazra et al., 2007). However, these authors determined that this was not a result of alterations in COX-2 expression, but rather involved induction of 15-hydroxyprostaglandin

dehydrogenase (PGDH), the enzyme that degrades PGE_2. One important difference in these two studies is the use of pharmacological agents to activate PPARγ. These drugs have off target effects, and thiazolidinediones have been shown to activate PGDH (Backlund et al., 2005), which would be predicted to decrease PGE_2 production. In our study, we have used a molecular approach by overexpressing PPARγ to achieve levels of activity comparable to what is achieved by thiazolidinedione stimulation (Bren-Mattison et al., 2005). Whether the effects in the study by Hazra et al are mediated through off-target mechanisms, or whether it reflects differences in the conditions used remains to be determined.

In conclusion, our data identify a link between PPARγ and COX-2 mediating the anti-tumorigenic effects of PPARγ. Furthermore, the activation of PPARγ will not only have direct effects on growth and transformation of NSCLC, but through inhibition of NF-κB will also disrupt tumor-stromal interactions required for progression and metastasis. We would propose that specific activators of PPARγ, such as thiazolidinediones will have both chemopreventive and chemotherapeutic effects in the treatment of NSCLC. Unfortunately, pharmacological PPARγ activators such as rosiglitazone and pioglitazone have recently been associated with increased cardiovascular risk (Lincoff et al., 2007). However, it is unclear whether the adverse effects are mediated through PPARγ-dependent pathways or through off-target effects of these drugs. Further studies comparing molecular overexpression of PPARγ with thiazolidinediones in NSCLC and other cell types are therefore required to determine whether second-generation PPARγ activators may be represent effective safer therapies.

MOL#42002

MOL#42002

References

Backlund MG, Mann JR, Holla VR, Buchanan FG, Tai H-H, Musiek ES, Milne GL, Katkuri S and DuBois RN (2005) 15-Hydroxyprostaglandin Dehydrogenase Is Down-regulated in Colorectal Cancer. *J Biol Chem* 280(5):3217-3223.

Berger J and Moller DE (2002) The mechanisms of action of PPARs. *Annu Rev Med* 53:409-435.

Blaine SA, Meyer AM, Hurteau G, Wick M, Hankin JA, Murphy RC, Dannenberg AJ, Geraci MW, Subbaramaiah K and Nemenoff RA (2005) Targeted over-expression of mPGES-1 and elevated PGE2 production is not sufficient for lung tumorigenesis in mice. *Carcinogenesis* 26(1):209-217.

Bren-Mattison Y, Van Putten V, Chan D, Winn R, Geraci MW and Nemenoff RA (2005) Peroxisome proliferator-activated receptor-gamma (PPAR(gamma)) inhibits tumorigenesis by reversing the undifferentiated phenotype of metastatic non-small-cell lung cancer cells (NSCLC). *Oncogene* 24(8):1412-1422.

Casibang M, Purdom S, Jakowlew S, Neckers L, Zia F, Ben-Av P, Hla T, You L, Jablons DM and Moody TW (2001) Prostaglandin E2 and vasoactive intestinal peptide increase vascular endothelial cell growth factor mRNAs in lung cancer cells. *Lung Cancer* 31(2-3):203-212.

Corti M, Brody AR and Harrison JH (1996) Isolation and primary culture of murine alveolar type II cells. *Am J Respir Cell Mol Biol* 14(4):309-315.

Debnath J, Muthuswamy SK and Brugge JS (2003) Morphogenesis and oncogenesis of MCF-10A mammary epithelial acini grown in three-dimensional basement membrane cultures. *Methods* 30(3):256-268.

Feige JN, Gelman L, Michalik L, Desvergne B and Wahli W (2006) From molecular action to physiological outputs: peroxisome proliferator-activated receptors are nuclear receptors at the crossroads of key cellular functions. *Prog Lipid Res* 45(2):120-159.

Gericke A, Munson M and Ross AH (2006) Regulation of the PTEN phosphatase. *Gene* 374:1-9.

Han S and Roman J (2006) Rosiglitazone suppresses human lung carcinoma cell growth through PPAR{gamma}-dependent and PPAR{gamma}-independent signal pathways. *Mol Cancer Ther* 5(2):430-437.

Hazra S, Batra RK, Tai HH, Sharma S, Cui X and Dubinett SM (2007) Pioglitazone and Rosiglitazone Decrease Prostaglandin E2 in Non-Small-Cell Lung Cancer Cells by Up-Regulating 15-Hydroxyprostaglandin Dehydrogenase. *Mol Pharmacol %R 101124/mol106033357* 71(6):1715-1720.

Heasley LE, Thaler S, Nicks M, Price B, Skorecki K and Nemenoff RA (1997) Induction of cytosolic phospholipase A$_2$ by oncogenic Ras in human non-small cell lung cancer. *J Biol Chem* 272:14501-14504.

Hida T, Leyton J, Makheja AN, Ben-Av P, Hla T, Martinez A, Mulshine J, Malkani S, Chung P and Moody TW (1998) Non-small cell lung cancer cyclooxygenase activity and proliferation are inhibited by non-steroidal antiinflammatory drugs. *Anticancer Res* 18(2A):775-782.

Horio Y, Chen A, Rice P, Roth JA, Malkinson AM and Schrump DS (1996) Ki-*ras* and *p53* mutations are early and late events, respectively, in urethane-induced pulmonary carcinogenesis. *Mol Carcinog* 17:217-223.

Huang C and Cabot MC (1990) Phorbol Diesters Stimulate the Accumulation of Phosphatidate, Phosphatidylethanol, and Diacylglycerol in Three Cell Types. *J Biol Chem* 265:14858-14863.

Inoue H, Tanabe T and Umesono K (2000) Feedback control of cyclooxygenase-2 expression through PPARgamma. *J Biol Chem* 275(36):28028-28032.

Keith RL, Miller YE, Hoshikawa Y, Moore MD, Gesell TL, Gao B, Malkinson AM, Golpon HA, Nemenoff RA and Geraci MW (2002) Manipulation of Pulmonary Prostacyclin Synthase Expression Prevents Murine Lung Cancer. *Cancer Res* 62(3):734-740.

Keshamouni VG, Arenberg DA, Reddy RC, Newstead MJ, Anthwal S and Standiford TJ (2005) PPAR-gamma activation inhibits angiogenesis by blocking ELR+CXC chemokine production in non-small cell lung cancer. *Neoplasia* 7(3):294-301.

Lee G, Elwood F, McNally J, Weiszmann J, Lindstrom M, Amaral K, Nakamura M, Miao S, Cao P, Learned RM, Chen J-L and Li Y (2002) T0070907, a Selective Ligand for Peroxisome Proliferator-activated Receptor gamma, Functions as an Antagonist of Biochemical and Cellular Activities. *J Biol Chem %R 101074/jbcM200743200* 277(22):19649-19657.

Lee SY, Hur GY, Jung KH, Jung HC, Lee SY, Kim JH, Shin C, Shim JJ, In KH, Kang KH and Yoo SH (2006) PPAR-gamma agonist increase gefitinib's antitumor activity through PTEN expression. *Lung Cancer* 51(3):297-301.

Lincoff AM, Wolski K, Nicholls SJ and Nissen SE (2007) Pioglitazone and Risk of Cardiovascular Events in Patients With Type 2 Diabetes Mellitus: A Meta-analysis of Randomized Trials. *Jama* 298(10):1180-1188.

Liu CH, Chang SH, Narko K, Trifan OC, Wu MT, Smith E, Haudenschild C, Lane TF and Hla T (2001) Overexpression of cyclooxygenase-2 is sufficient to induce tumorigenesis in transgenic mice. *J Biol Chem* 276(21):18563-18569.

Madrid LV, Wang CY, Guttridge DC, Schottelius AJ, Baldwin AS, Jr. and Mayo MW (2000) Akt suppresses apoptosis by stimulating the transactivation potential of the RelA/p65 subunit of NF-kappaB. *Mol Cell Biol* 20(5):1626-1638.

Malkinson AM (1998) Molecular comparison of human and mouse pulmonary adenocarcinomas. *Exp Lung Res* 24(4):541-555.

McLemore TL, Hubbard WC, Litterst CL, Lin MC, Miller S, McMahon NA, Eggleston JC and Boyd MR (1988) Profiles of prostaglandin biosynthesis in normal lung and tumor tissue from lung cancer patients. *Cancer Res* 48:3140-3147.

Meyer AM, Dwyer-Nield LD, Hurteau GJ, Keith RL, O'Leary E, You M, Bonventre JV, Nemenoff RA and Malkinson AM (2004) Decreased lung tumorigenesis in mice genetically deficient in cytosolic phospholipase A2. *Carcinogenesis* 25(8):1517-1524.

Moody TW, Leyton J, Zakowicz H, Hida T, Kang Y, Jakowlew S, You L, Ozbun L, Zia H, Youngberg J and Malkinson A (2001) Indomethacin reduces lung adenoma number in A/J mice. *Anticancer Res* 21(3B):1749-1755.

Patel L, Pass I, Coxon P, Downes CP, Smith SA and Macphee CH (2001) Tumor suppressor and anti-inflammatory actions of PPARgamma agonists are mediated via upregulation of PTEN. *Curr Biol* 11(10):764-768.

Reddy ST, Wadleigh DJ and Herschman HR (2000) Transcriptional regulation of the cyclooxygenase-2 gene in activated mast cells. *J Biol Chem* 275(5):3107-3113.

Rigas B and Kashfi K (2005) Cancer prevention: a new era beyond cyclooxygenase-2. *J Pharmacol Exp Ther* 314(1):1-8.

Romashkova JA and Makarov SS (1999) NF-kappaB is a target of AKT in anti-apoptotic PDGF signalling. *Nature* 401(6748):86-90.

Sasaki H, Tanahashi M, Yukiue H, Moiriyama S, Kobayashi Y, Nakashima Y, Kaji M, Kiriyama M, Fukai I, Yamakawa Y and Fujii Y (2002) Decreased perioxisome proliferator-activated receptor gamma gene expression was correlated with poor prognosis in patients with lung cancer. *Lung Cancer* 36(1):71-76.

Sizemore N, Leung S and Stark GR (1999) Activation of phosphatidylinositol 3-kinase in response to interleukin-1 leads to phosphorylation and activation of the NF-kappaB p65/RelA subunit. *Mol Cell Biol* 19(7):4798-4805.

Strieter RM, Belperio JA, Burdick MD, Sharma S, Dubinett SM and Keane MP (2004) CXC chemokines: angiogenesis, immunoangiostasis, and metastases in lung cancer. *Ann N Y Acad Sci* 1028:351-360.

Teresi RE, Shaiu CW, Chen CS, Chatterjee VK, Waite KA and Eng C (2006) Increased PTEN expression due to transcriptional activation of PPARgamma by Lovastatin and Rosiglitazone. *Int J Cancer* 118(10):2390-2398.

Theocharis S, Kanelli H, Politi E, Margeli A, Karkandaris C, Philippides T and Koutselinis A (2002) Expression of peroxisome proliferator activated receptor-gamma in non-small cell lung carcinoma: correlation with histological type and grade. *Lung Cancer* 36(3):249-255.

Van Putten V, Refaat Z, Dessev C, Blaine S, Wick M, Butterfield L, Han SY, Heasley LE and Nemenoff RA (2001) Induction of Cytosolic Phospholipase A2 by Oncogenic Ras Is Mediated through the JNK and ERK Pathways in Rat Epithelial Cells. *J Biol Chem* 276(2):1226-1232.

Wick M, Hurteau G, Dessev C, Chan D, Geraci MW, Winn RA, Heasley LE and Nemenoff RA (2002) Peroxisome Proliferator-Activated Receptor-gamma Is a Target of Nonsteroidal Anti-Inflammatory Drugs Mediating Cyclooxygenase-Independent Inhibition of Lung Cancer Cell Growth. *Mol Pharmacol* 62(5):1207-1214.

Xie W and Herschman HR (1995) *v-src* induces prostaglandin synthase 2 gene expression by activation of the c-Jun N-terminal kinase and the c-Jun transcription factor. *J Biol Chem* 270:27622-27628.

Current Address for Y B-M: Sporian Microsystems Inc.
515 Courtney Way
Lafayette, CO 80026

Footnotes
1. These authors contributed equally to this work.

2. Van Putten, V, Heasley, L.E., and Nemenoff, R.A. unpublished observations.

MOL#42002

Figure Legends

Figure 1   Effect of PPARγ on COX-2 Expression and PGE$_2$ Production

H2122-LNCX (LNCX) or H2122-PPARγ (PPARγ) cells were grown under standard conditions. **A.** Cell lysates were prepared in RIPA buffer and equal amounts of protein were immunoblotted for cPLA$_2$, COX-2, and mPGES. Levels of both COX-2 and cPLA$_2$ were decreased in H2122-PPARγ cells. Data show is a representative blot of three independent experiments. **B.** Conditioned medium from 90% confluent dishes of H2122-LNCX, or H2122-PPARγ treated overnight with either vehicle or 10μM T007 was collected after a one-hour incubation and assayed for PGE$_2$ production by ELISA. The cells on the dish were harvested and total protein determined. PGE$_2$ production was normalized to cell protein. Results represent the mean of 3 independent experiments with the SEM indicated. **C.** Cells were transfected with a construct encoding 500 bp of the human COX-2 promoter linked to a luciferase reporter, along with a construct encoding β-galactosidase under the control of the CMV promoter to normalize for transfection efficiency. Five hours after transfection, cells were treated with 10μM T007, or vehicle (DMSO, final concentration 0.1%. Cells were harvested after 24 hours and luciferase activity normalized to β-gal determined. Results represent the mean of 3 independent experiments with the SEM indicated. *P<0.05 vs LNCX

Figure 2   PGE$_2$ Reverses the Effects of PPARγ in 3-D Culture

H2122-LNCX or H2122-PPARγ cells were grown in 3-D Matrigel culture as described in the Methods Section for 8-10 days. For cells treated with either sulindac sulfide or PGE$_2$, drugs were added to the Matrigel at time of plating (5 μM of each drug) and replaced with each feeding of the cells. Cells were visualized under phase at low power (Panels A-D). Cells were then fixed and stained for E-cadherin expression (Green), activated caspase (Red), or DAPI (Blue) as described in the Methods Section.

Representative acinar structures are shown in Panels E-H. H2122-PPARγ (Panels B,F) cells formed regular acinar structures compared to H2122-LNCX(Panels A, E). Sulindac sulfide caused LNCX cells to adopt a more highly differentiated morphology (Panel C,G). Conversely, addition of exogenous PGE$_2$ caused PPARγ cells to adopt a more de-differentiated morphology.

Figure 3   PPARγ Inhibits NF-κB Activity

A.   H2122-LNCX and H2122-PPARγ cells were transiently transfected with an NF-κB-luciferase construct along with CMV-βgal to normalize for transfection efficiency. Cells were then treated with 10 μM T007 or vehicle and incubated for 24 hours. Extracts were assayed for luciferase and β-gal activity. Luciferase activity was decreased in H2122-PPARγ cells, and this effect was blocked in the presence of the PPARγ inhibitor. Results represent the mean of 4 independent experiments. *B.* NF-κB activity was assayed in H2122-LNCX cells and H2122-PPARγ cells by ELISA. Nuclear extracts were prepared from each cell type using the Active Motif nuclear extract kit, and assayed for activity with the TransAM NF-κB chemiluminescence kit from Active Motif. Results represent the mean of 2 independent experiments. *P<0.05 vs LNCX Cells

Figure 4   PPARγ Inhibition of NF-κB Blocks COX-2 Expression in NSCLC

A. H2122 cells were transiently transfected with either the NF-κB luc reporter (left bars) or the COX-2-promoter construct (right bars) along with an expression plasmid encoding DN-IκB, or empty vector (pcDNA-3) *B.* H2122 cells were transfected with the NF-κB-luciferase reporter. Five hours after transfections cells were exposed to the indicated concentration of the IKK inhibitor. After 24 hours, cells were harvested and luciferase activity normalized to β-gal was determined. Results **for both A and B** represent the mean of three independent experiments with the SEM indicated. *P<0.05 vs no

27

drug; **P<0.01 vs no drug. ***C.*** H2122 cells were exposed for 24 hours to the indicated concentration of the IKK inhibitor or vehicle (0.1% DMSO). Cell lysates were prepared, and immunoblotted for COX-2 expression. Lysates were blotted for β-actin as a loading control. Results are representative of 3 independent experiments.

Figure 5 PPARγ Expression Inhibits NF-κB Activity and COX-2 Promoter in A549 Cells

A549 cells were transiently transfected with either the NF-κB luc reporter (***Panel A***) or the COX-2-promoter construct (***Panel B***) along with either an expression plasmid encoding full-length PPARγ or a control plasmid (pcDNA-3). Expression of PPARγ decreased both NF-κB-luc and COX-2 luc activity. All experiments represent the mean of at least 3 independent experiments with the SEM indicated. *P<0.05 vs pcDNA-3.

Figure 6 PPARγ Effects on NFκB are mediated through Activation of PTEN and Leading to Inhibition of Akt

A. Cells lysates were prepared from H2122-LNCX and H2122-PPARγ cells and immunoblotted for phospho-Akt (p-Akt) or total Akt. A representative blot is shown. ***B.*** H2122-LNCX and H2122-PPARγ cells were transiently transfected with the NF-κB-luciferase reporter along with CMV-β-gal encoding plasmid to normalize for transfection efficiency. After 16 hours, cells were treated with 10 μM LY 294402 or vehicle (0.1% DMSO) for an additional 48 hours. Luciferase activity normalized to β-gal was determined. Data represent the mean of 3 independent experiments with the SEM indicated. ***C.*** Cell lysates from H2122-LNCX or H2122-PPARγ cells were immunoprecipitated with anti-PTEN antibody. Extracts were also immunoprecipitated with normal IgG as a negative control. Phosphatase

activity against PIP_3 was determined in the immunoprecipitate, and quantitated using a phosphatase assay kit from Echelon. Data represent the mean of 2 independent experiments with the SEM indicated.

Figure 7   Mice with Targeted Overexpression of PPARγ Are Protected Against Lung Tumorigenesis

Transgenic mice overexpressing PPARγ under the control of the surfactant protein C promoter were developed as described in the methods section. Mice were genotyped as previously described (Blaine et al., 2005), and propagated as heterozygotes in the FVB strain. ***Panel A.*** Type II pneumocytes were isolated from Tg+ mice and wild type littermates. Cell lysates were immunoblotted for PPARγ and COX-2. PPARγ expression was markedly increased in the Tg+ mice; the lower band in the immunoblot is a non-specific band. COX-2 levels were decreased in extracts of Type II cells. ***Panel B.*** Equal numbers of PPARγ-Tg+ mice and wild-type littermates (10/group) were injected with urethane as previously described (Blaine et al., 2005). After 18 weeks, animals were sacrificed, lungs removed and tumor number and size quantitated using a dissecting microscope. PPARγ-Tg+ mice had 75% fewer tumors. *P<0.05. ***Panel C***. Sections showing urethane-induced tumors after 18 weeks at 40x magnification: *Right*-Wild-type mice; *Left*- PPARγ-Tg+ mice.

Figure 1

Figure 2(A-D)

Figure 2 (E-H)

E

F

LNCX

PPARγ

G

H

LNCX + Sulindac Sulfide

PPARγ + PGE$_2$
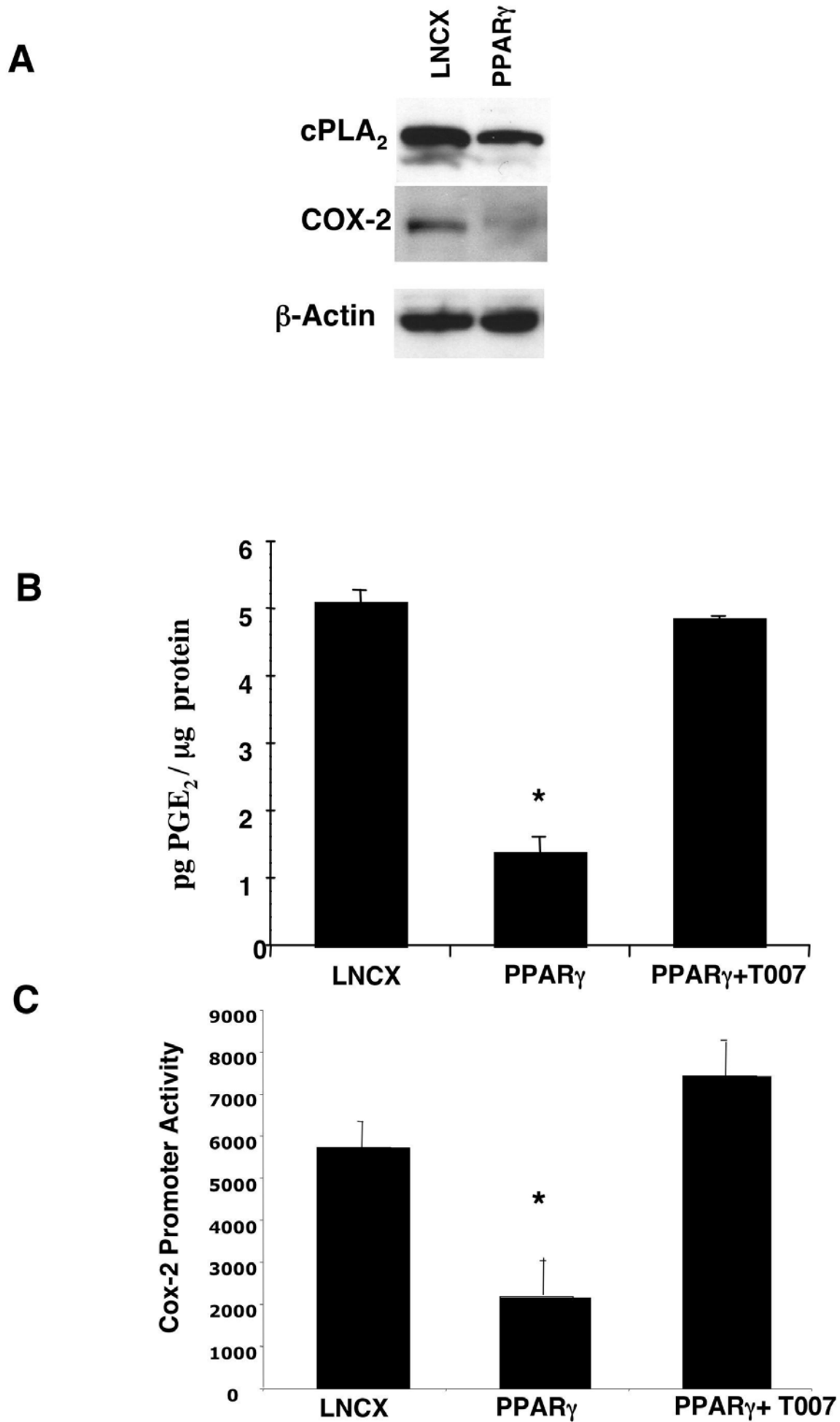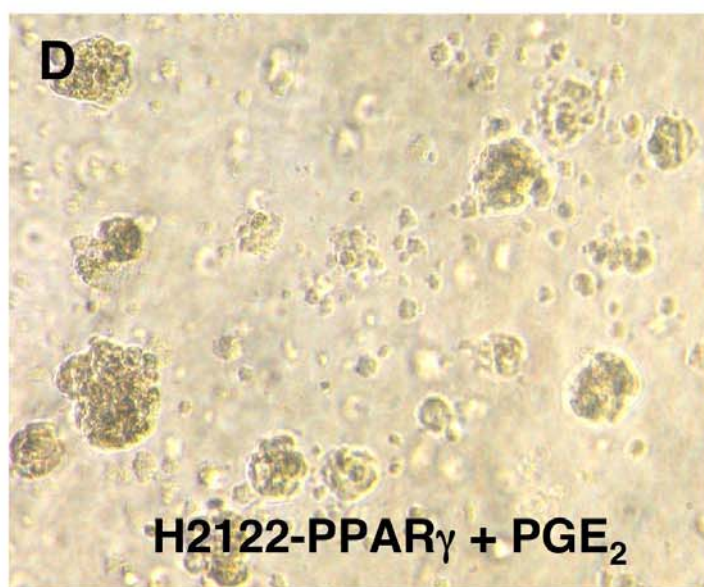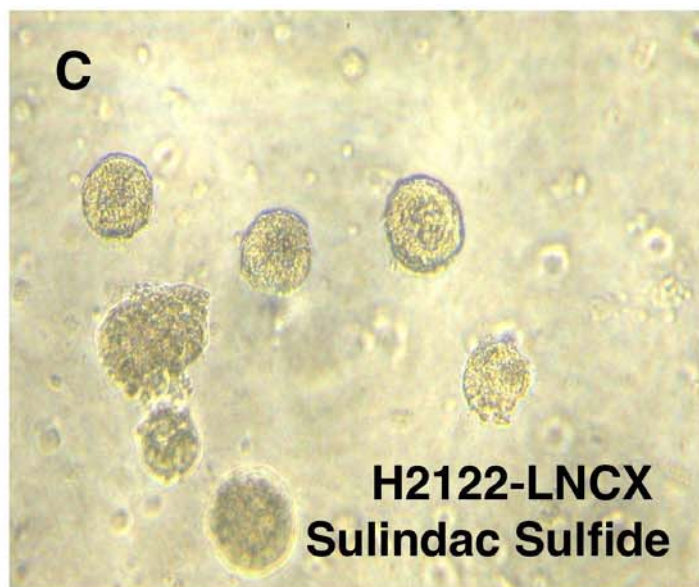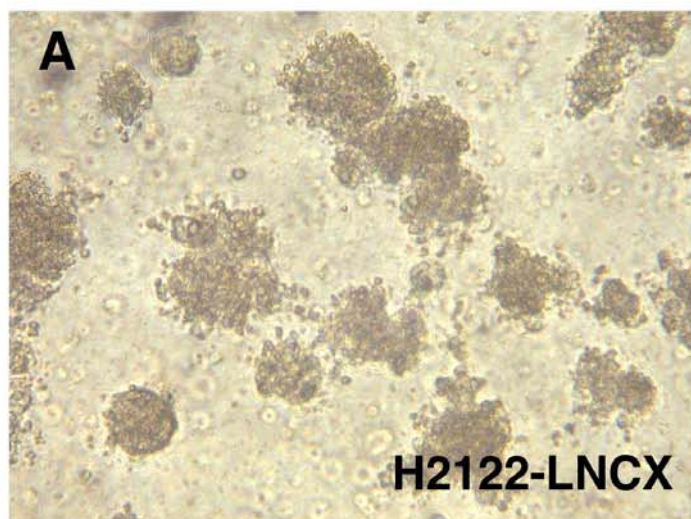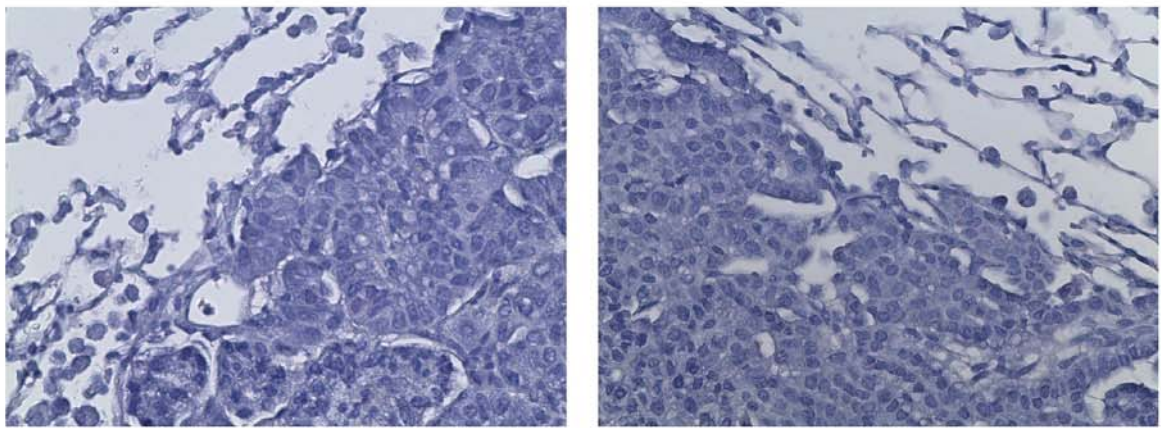
Figure 3
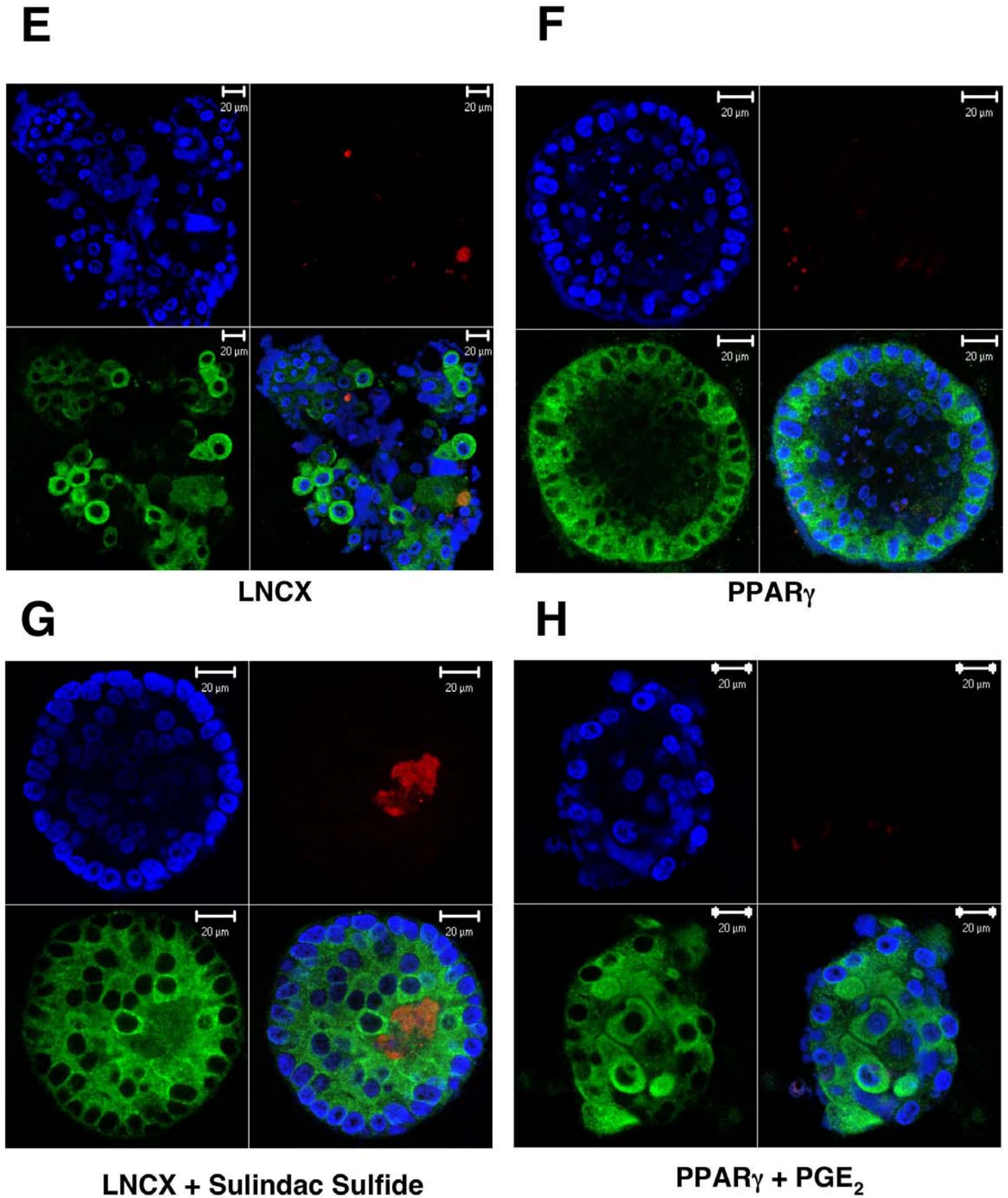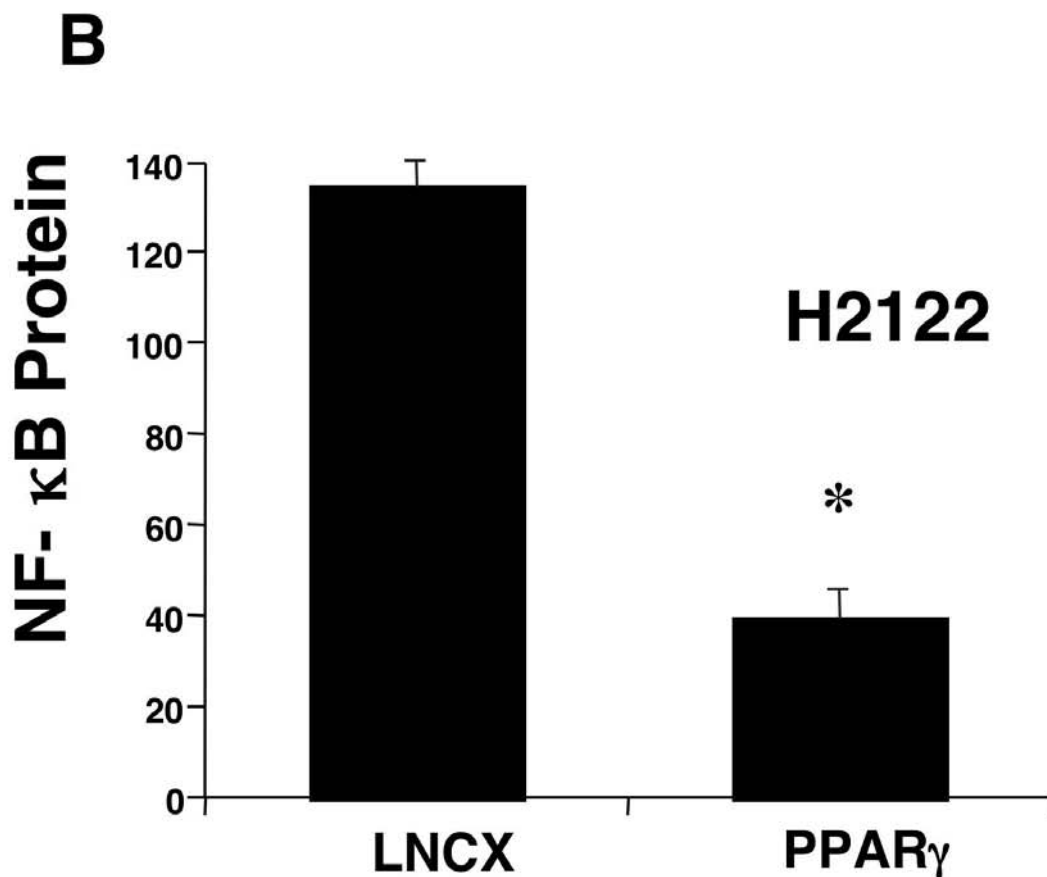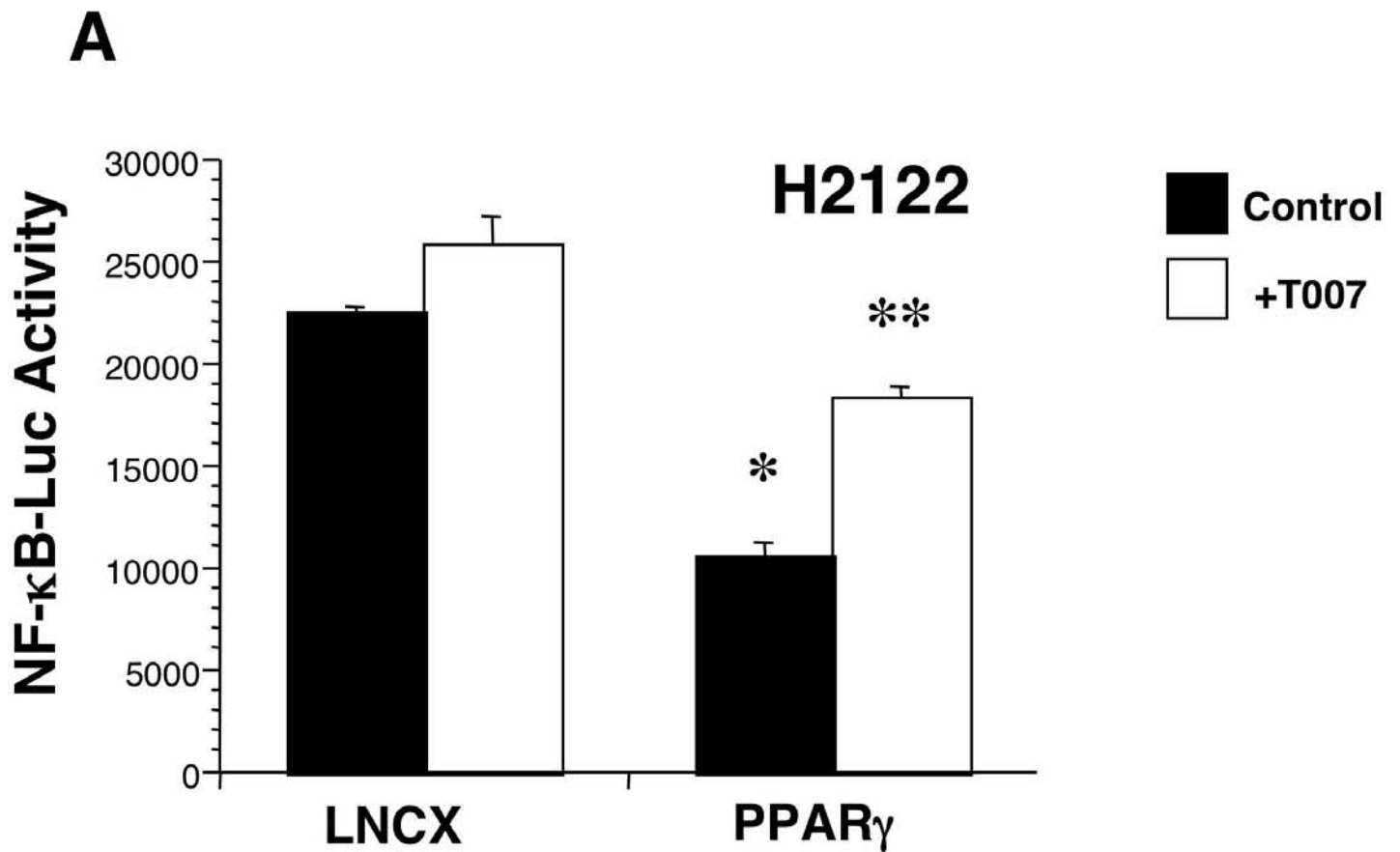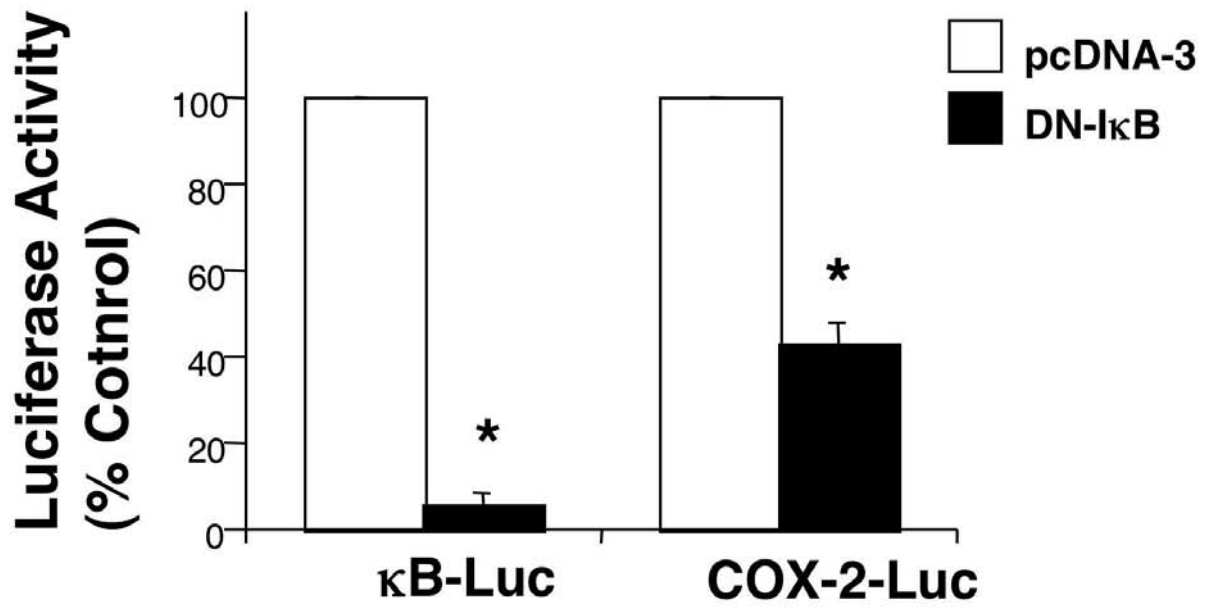
Figure 4
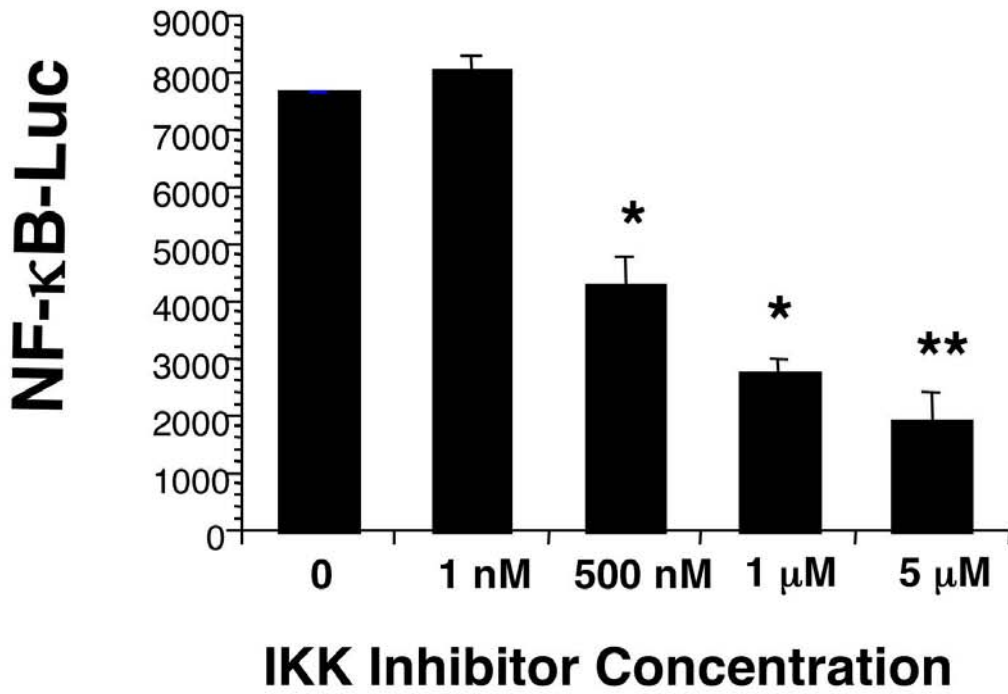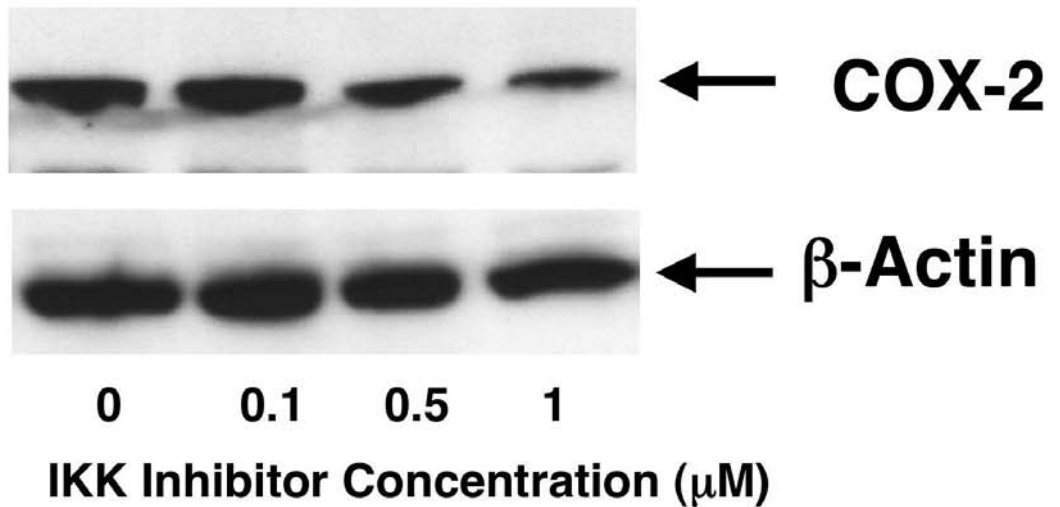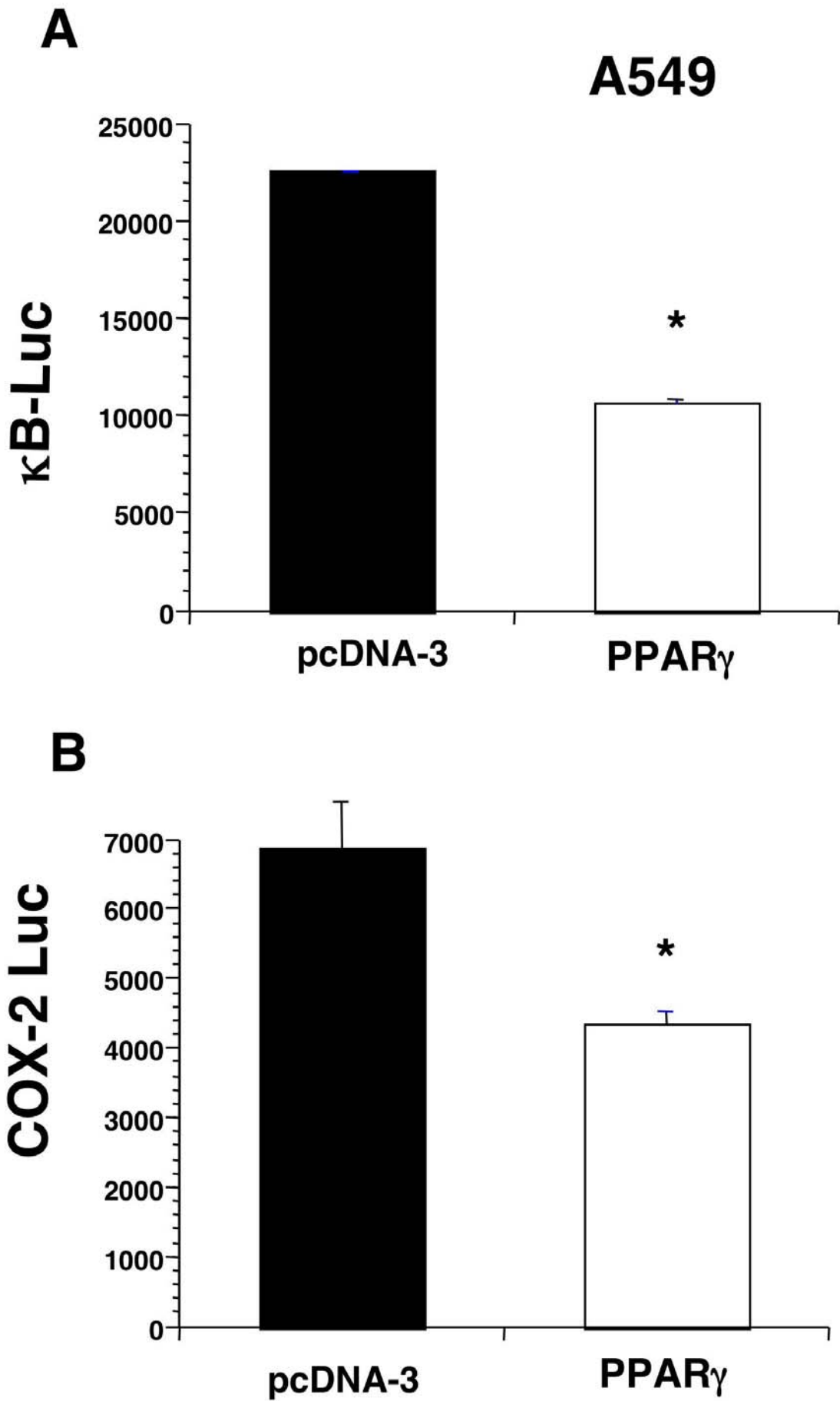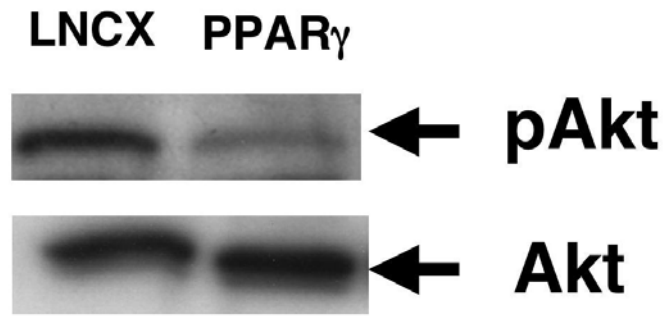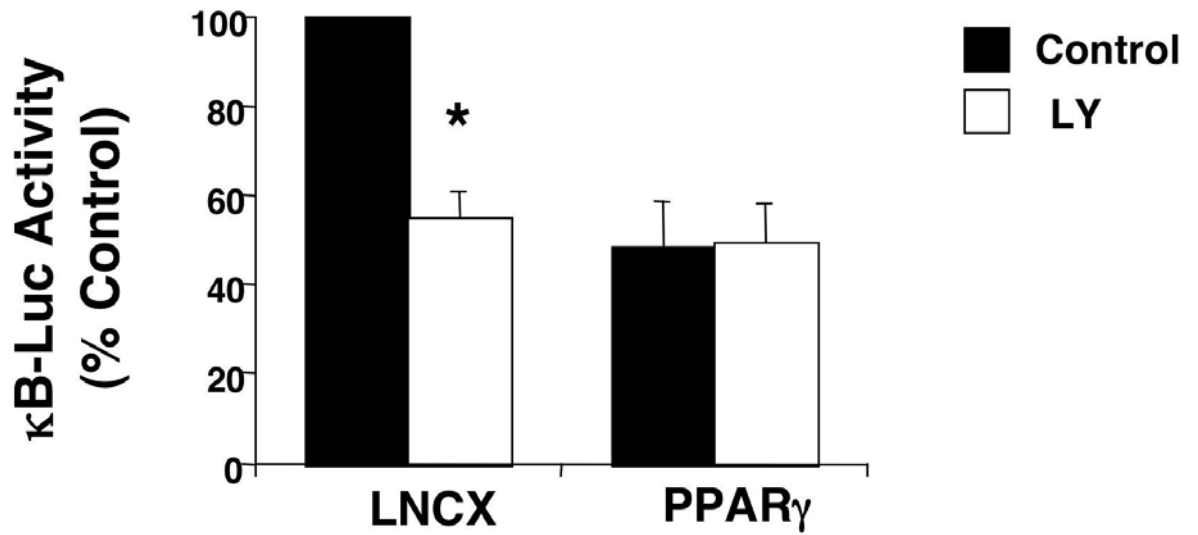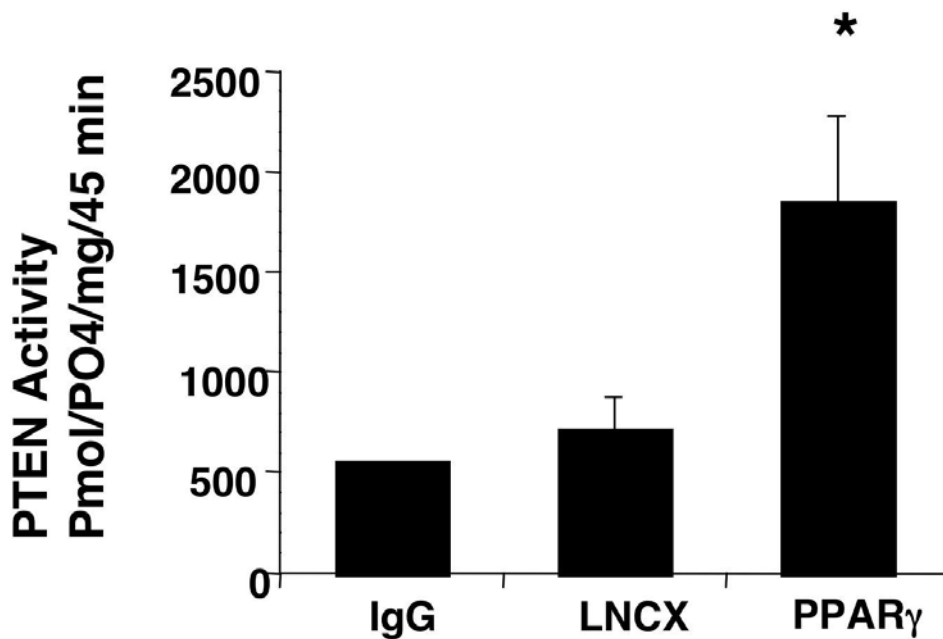
Figure 5

Figure 6

Figure 7

A

B

C

Wild-Type   PPARγ-Tg+